Journal of the European Ceramic Society 18 (1998) 1571–1578

PII: S0955-2219(98)-00017-X
0955-2219/98/$—see front matter

Grain Boundary Blocking Effect in Tetragonal Yttria Stabilized Zirconia

A. P. Santos,[a] R. Z. Domingues[b] and M. Kleitz[a]*

[a]Laboratoire d'Electrochimie et de Physicochimie des Materiaux et des Interfaces, INPG and CNRS, BP 75, 38402 Saint-Martin d'Hères, France
[b]Departamento de Quimica, Universidade Federal de Minas Gerais, C.P. 702, 31270-901 Belo Horizonte, MG, Brazil

(Received 12 August 1997; revised version received 5 January 1998; accepted 23 January 1998)

Abstract

Abstract samples of yttria stabilized tetragonal zirconia, with different grain sizes have been synthesized. Care was taken to avoid the presence of any trace of monoclinic zirconia. The features of their grain boundary blocking effect are compared to those of YSZ samples of similar purity. Certain variation laws of the blocking effects are quasi identical, especially some dependences on the grain size. The most significant differences concern the variation of the blocking factor with temperature and the transition to the so-called intrinsic regime. In tetragonal zirconia, the blocking factor continuously decreases in the temperature interval 150–600°C and the onset of the intrinsic regime could occur at a smaller grain size of about 0·9 μm. © *1998 Elsevier Science Limited. All rights reserved*

Keywords: TZP, grain growth, grain boundaries, blocking effect, impedance spectroscopy.

1 Introduction

Recent results[1] obtained on dense cubic yttria stabilized zirconia (YSZ) have shown that interesting correlations can be established between the average grain size of the material and parameters of the grain boundary blocking effect. These correlations could reveal specific features of the grain boundary microstructure. The search for similar correlations in materials chemically or structurally related to YSZ is one of the motivations of this study of the grain boundary blocking effect in yttria stabilized tetragonal zirconia polycrystalline (Y-TZP). Another investigation[2] has shown that the impedance spectroscopy is a powerful tool for the phase change characterization in moderately conducting materials. Its implementation to the tetragonal zirconia destabilization, that has already been examined[3,4] and that will be the subject of a second paper, requires a detailed characterization of the blocking effect of the material before destabilization. This is the second motivation for our investigation.

A third motivation is technological: it is generally agreed that a drawback of tetragonal zirconia for electrical applications, would be its important grain boundary blocking effect. It certainly is related to the small grain size of this material, but is it only due to that? Could it be a specific property of the tetragonal zirconia grain boundaries? This question also deserved to be tackled.

The characterization by impedance spectroscopy of the electrical properties of tetragonal zirconia has already been the subject of several investigations by the groups lead by Steele[5,6] Badwal[7–15] and by others.[16–21] The main conclusions are:

- Two fairly well defined semicircles can easily be separated on the impedance diagrams. As in the case of YSZ, they have been ascribed to the intragrain properties (here, identified by the indice: bulk) and to blocking effects at the grain boundaries (indice: blocked).
- The grain boundary semicircle markedly depends on the content of insoluble impurities in the material. Silica is a strong blocking agent.
- In the impure materials the blocking effect is drastically reduced by quenching the material from the sintering temperature (or from a sufficiently high annealing temperature). In the 'pure' Y-TZP, (containing less than 50 ppm of SiO_2) this quenching influence is far less pronounced.

*To whom correspondence should be addressed.

- The specific (bulk) resistivity was also found to vary noticeably on quenching.
- A segregation of yttrium along the grain boundaries has frequently been observed and quantitatively measured. It is regarded as being most likely responsible for the blocking effect in nominally pure Y–TZP. This statement is supported by microscopic investigations[22–26] which have shown grain boundaries free of any second phase although they were found partly blocking.

2 Experimental

The investigated material (TZ-3Y from TOSOH Corp., lot no. Z30020SP) is stabilized in its tetragonal phase by 2·8 mol% Y_2O_3 and contains approximately the same contents of impurities as the cubic zirconia to which our results will be compared. The supplier quotes a silica content lower than 20 ppm (in wt%). The other impurity contents are listed in Table 1.

To avoid any contamination, the samples were manipulated as little as possible. They were first uniaxially pressed under 35 MPa, then isostatically pressed under 250 MPa and sintered in air, in two steps (pre-sintering and sintering steps) of 1 and 3 h, respectively, at the temperatures shown in Table 2.

The heating and cooling rates were 100°C h^{-1}. Some samples were cooled at 300°C h^{-1} after annealing at 1300°C for 1 h. After the pre-sintering stage (at either 1350 or 1500°C), the samples were accurately shaped with diamond tools to pellets 8 mm in diameter and 3 mm high and then further sintered to their final sintering temperature (see Table 2). This procedure eliminated the monoclinic phase produced by the machining of the samples.[27] The absence of monoclinic phase in the bulk of the samples was checked by X-ray diffraction analysis using the low angle $(111)m$, $(111)_t$ and $(111)_m$ reflexions, after elimination of a thin surface layer by gentle polishing. This procedure was applied because traces of surface monoclinic phase can result from the interaction of the sample with humid air at medium temperature. (These can also be eliminated by annealing at 600°C in dry air).

For the microstructure analysis (JEOL JSM 6400), the sample surfaces were polished with SiC papers (grades 600 and 1000) and diamond pastes down to 1 μm. The microstructure was revealed by thermal etching for 30 mn at about 100°C below the final sintering temperature. The grain size distributions were determined with the computer code 'NIH Image' (US National Institute of Health). The diameters obtained with this code were multiplied by $4/\pi$ to get a better evaluation of the real grain diameter, under the spherical grain approximation.

Table 1. Impurity contents

Impurities	SiO_2	Al_2O_3	Fe_2O_3	Na_2O
Contents (wt%)	< 0·002	< 0·005	0·002	0·027

Table 2. Pre-sintering and sintering temperatures

Pre-sintering temperature (°C)	1350	1350	1350	1500	1500	1500	1500	1500
Sintering temperature (°C)	1350	1400	1450	1500	1550	1600	1625	1650

For the impedance spectroscopy, silver coatings (Demetron silver paint no. 200) baked at 650°C for 1 h, in air, were used as electrodes. The impedance diagrams (Helwett–Packard impedancemeter HP 4192A) were recorded in the 5·1·3×10^7 Hz frequency-range, with a 150 mV signal amplitude. Most of the diagrams were recorded at 350 and 450°C where the maximum accuracy is obtained for the blocking effect parameters. Some measurements were carried out every 50°C from 200 to 600°C. The diagram resolution was performed with a computer code developed for HydroQuebec (Canada). The diagrams reported here are normalized to a unit geometrical factor and the electrode loops have been subtracted. As will be seen below, the diagrams obtained are all composed of two component semicircles. They describe the specific response of the intragrain material and of the blocking effect at the grain boundaries. From each semicircle were deduced: a conductivity σ (or resistivity ρ), a relaxation frequency F^O, a capacitive effect C and a depression angle β. For the reasons given in the reference papers,[28,29] the bulk parameters σ_{bulk}, F^0_{bulk}, C_{bulk} were deduced from the bulk component of the impedance diagrams (this evaluation is equivalent to that which can be made from the corresponding admittance diagrams, but practically it is more accurate). On the other hand, the blocking effect parameters $\sigma_{blocked}$, $F^0_{blocked}C_{blocked}$ were deduced from the corresponding admittance diagrams. Their values can be noticeably different from those calculated from the impedance diagrams and that mode of evaluation is more consistent with our model.[29] From these parameters we have calculated relative parameters to characterize the blocking effect. They are defined by the following equations:

$$\alpha_R = \sigma_{blocked}/\sigma_{bulk},\ \alpha_F = F^0_{blocked}/F^0_{bulk},\ \alpha_C = C_{blocked}/C_{bulk} \quad (1)$$

They are called, respectively, the blocking factor (α_R), the frequency ratio (α_F) and the capacitance ratio (α_C).

The use of such normalized parameters allows us to compare the blocking effects of various materials and the comparison is fairly independent from the model referred to. The blocking process could be due to a continuous low conductivity 'film' covering the grains (film made of an impurity phase or formed by the grain sub-layers enriched in the matrix dopant) or to discontinuous insulating 'inclusions' (made of an impurity phase or simply of voids). Our model is of the latter type. The basic idea is that the inclusions statistically block a part of the matrix carriers, at sufficiently low frequency. The associated 'blocked' conductivity is in parallel to the conductivity associated to the free matrix carriers. For more detail on this diagram resolution and on the relevant bibliography, the reader is referred to Ref. 29.

3 Material characterization

The samples sintered above 1400°C are virtually fully dense (relative density higher than 99%), in agreement with results[15,30–33] already published. That sintered at 1350°C is slightly porous (density of 98%). The SEM micrographs (Fig. 1) of all the samples show fairly narrow grain size distributions. Figure 2 gives the Arrhenius diagram of the average grain sizes. The corresponding activation energy is 1·6 eV, much smaller than the 3·0 eV value recently measured[1] for YSZ (8 mol% Y_2O_3). This is in qualitative agreement with the common observation that grain growth is much slower in Y-TZP than in YSZ. The sintering in two steps that was applied here, cannot be regarded as the cause of this significant difference. Most certainly, it indicates a major difference in the sintering mechanism, either in the magnitude of a determining step or in its nature. This should be related to differences in the grain boundary morphology.

Figure 3 shows two typical impedance diagrams. All the diagrams which were recorded were shaped like these and their resolution was without ambiguity and accurate to within 1%. Figure 3 also compares them to those of YSZ samples of similar grain sizes and of similar impurity levels. They are remarkably similar. This similarity will be examined in detail below.

To further ensure that all the investigated samples are composed solely of tetragonal zirconia and that no monoclinic precipitates interfere with the measurements, we referred to the following results.

- The resistivities deduced from the bulk semicircles are virtually independent of the sintering temperature. Figure 4 shows the variations of this parameter relative to the average value

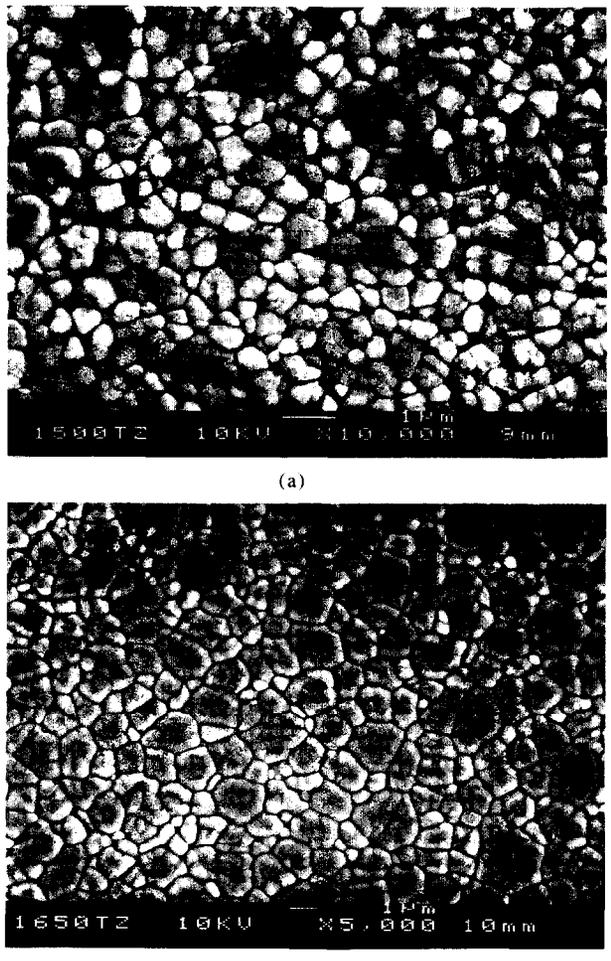

Fig. 1. Scanning electron micrographs of samples sintered at (a) 1500°C and (b) 1650°C.

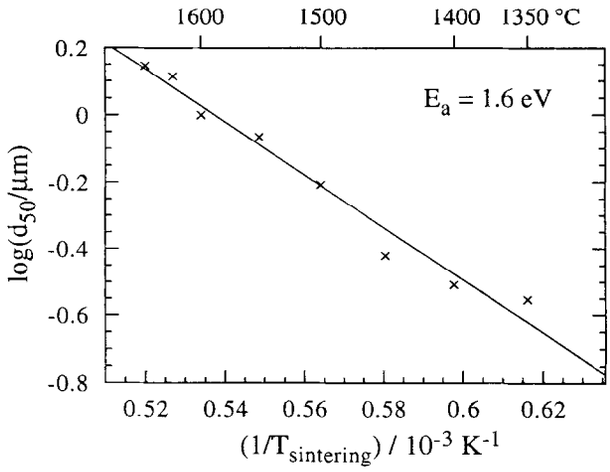

Fig. 2. Arrhenius diagram of the average grain size.

obtained in the sintering temperature range 1500–1650°C. The variations remain small and of the order of the experimental uncertainty except for sintering temperatures lower than 1450°C. In these materials, the risk of the presence of monoclinic phase is quasi nill because of the small grain size (about 0·3 μm). The observed increase in the resistivity, of the order of 10%, could be partially due to the

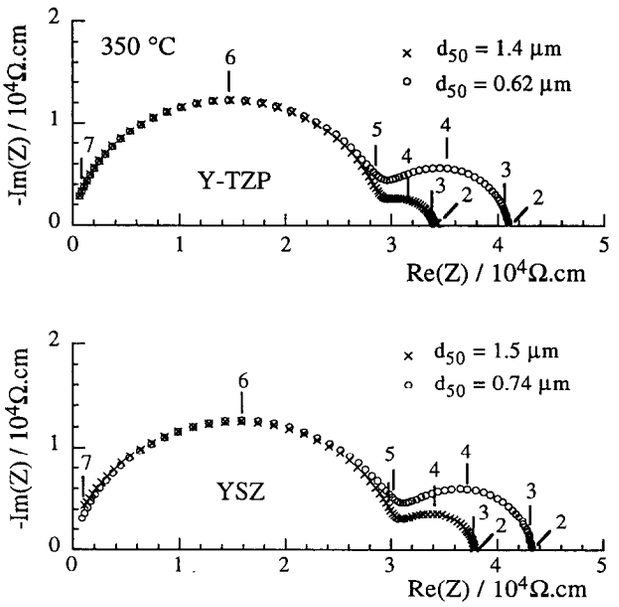

Fig. 3. Impedance diagrams of TZP with different grain sizes: 1·4 and 0·62 μm. Comparison with diagrams[1] of YSZ of similar grain sizes (1·5 and 0·74 μm).

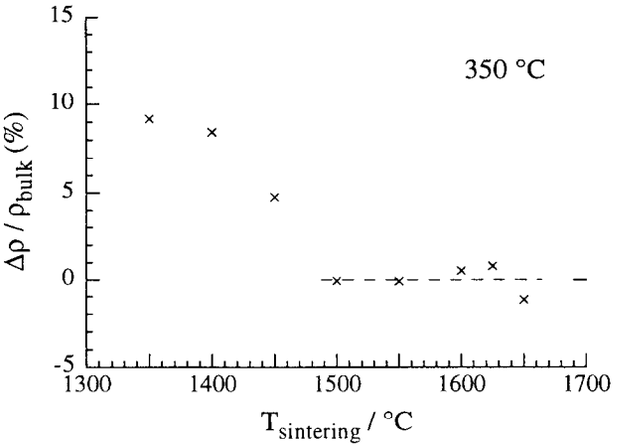

Fig. 4. Relative variations of the bulk resistivity as a function of the sintering temperature. (Measurement temperature: 350°C.)

influence of the porosity. In a previous study[1] of the influence of the porosity on the bulk conductivity/resistivity, the following equation was established:

$$\sigma_{bulk} = \sigma^0_{bulk}\langle 1 - P\rangle^{2.74} \qquad (2)$$

where σ_{bulk} is the conductivity measured for the sample of porosity P and σ^0_{bulk} that of a fully dense material. The application of this equation gives a variation of only 6% for σ_{bulk} which is slightly smaller than observed.

- The depression angles (Fig. 5) which are parameters sensitive to the heterogeneity of the material are small compared to the usual values (especially the blocking effect angle) and virtually constant.
- The bulk relaxation frequency (Fig. 6), at a given temperature, is also virtually independent of the sintering temperatures.

The presence of monoclinic zirconia would have resulted in an additional semicircle as previously demonstrated[2] in the case of ZrO_2-MgO. This semicircle could either be directly visible, which is not the case in our results, or masked by interference with either the bulk or the grain-boundary semicircle. This would have been revealed by an abnormal variation of the semicircle parameters. The small value of the blocking effect depression angle shows that there is no overlapping with the grain boundary semicircle. The small (and regular) relative variations of the bulk relaxation frequency indicates that neither is the case for the bulk semicircle.

Figure 7 shows the Arrhenius diagram of the bulk conductivity and those of the blocked conductivities of two samples of different grain sizes (1·3 and 0·28 μm). The corresponding activation energies are 0·84 eV for the bulk conductivity and

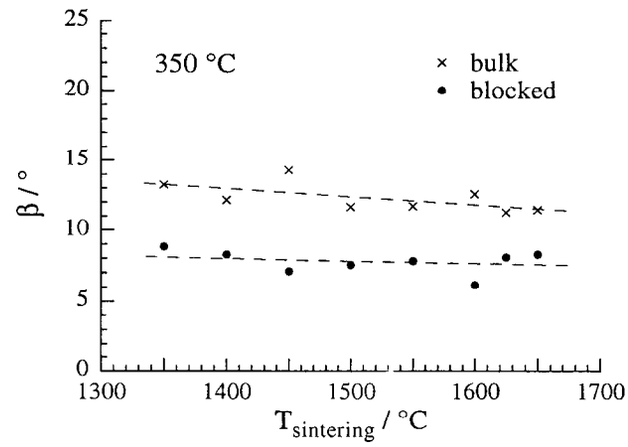

Fig. 5. Variations of the depression angles as functions of the sintering temperature.

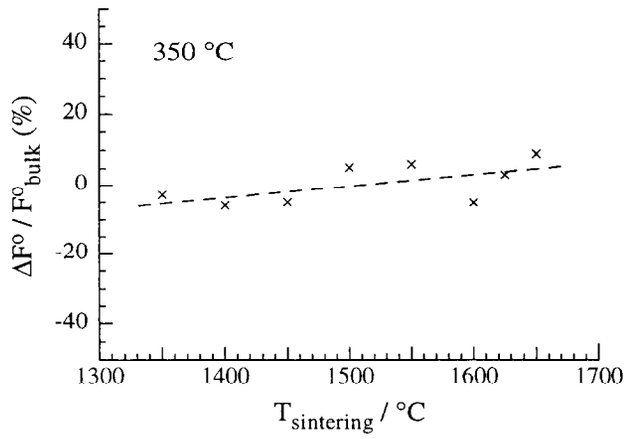

Fig. 6. Relative variations of the bulk relaxation frequency as a function of the sintering temperature.

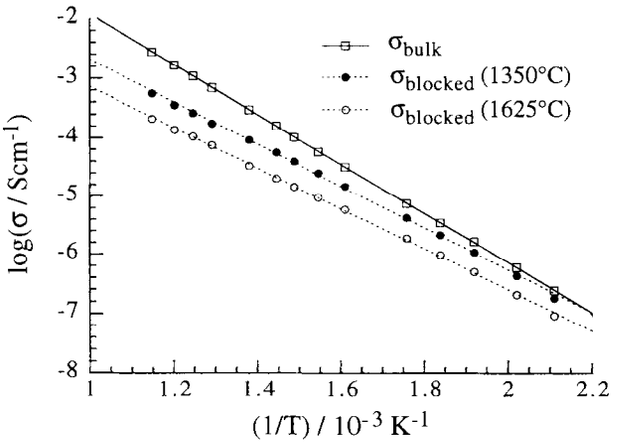

Fig. 7. Arrhenius diagram of the bulk conductivity and of the blocked conductivities of samples sintered at 1350 and 1625°C.

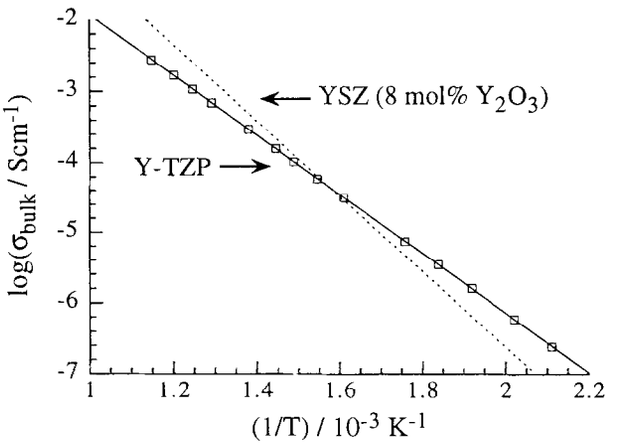

Fig. 8. Comparison of the bulk conductivity Arrhenius diagrams of Y-TZI and YSZ.

0·68 and 0·71 eV for the blocked conductivity, over the investigated temperature domain. To give an estimate of the current scattering in the bulk properties, Table 3 compares the literature data on the activation energy and the value at 350°C of the bulk conductivity.

As frequently noted for other materials, the activation energies obtained for the blocked conductivities (deduced from the corresponding admittance diagrams) are smaller than the bulk property. The results cannot easily be compared to the literature data because the reference models and the calculation mode are different. (A few calculations made according to the more conventional 'series' model gave results similar to the published data.)

Figure 8 compares the bulk conductivity of the investigated tetragonal zirconia to that[1] of the YSZ stabilized with 8 mol% Y_2O_3. Both conductivities are equal at 390°C. Badwal[8,12] noted that at 400°C the conductivities of these two materials are very close.

The bulk dielectric constant calculated from the bulk semicircle, over the investigated sintering temperature interval, is shown in Fig. 9. It is constant and the average value is 60. This value was found independent of the measurement temperature. It is very similar to the YSZ dielectric constant determined under the same conditions.[1] (Note that at room temperature, where the electric conductivity is virtually nil, the dielectric constant was found[1] different for YSZ.)

4 Impedance diagram analysis

According to our usual presentation[1,2,34] of the blocking features, Figs 10 and 11. first show the variations of the blocking factor and of the frequency factor over the measurement temperature. In marked contrast with the corresponding results reported for YSZ (and with most of the other reported relevant features), the curves do not show any plateau where the parameters can be determined independently of the measurement temperature. The blocking factor of the YSZ has also been observed to significantly decrease with temperature, but only above a certain critical temperature (of the order of 550°C). This decrease has been interpreted[29] as a consequence of increase in the matrix conductivity with temperature: the higher the matrix conductivity, the closer the current lines run around the blockers and therefore the smaller the fraction of the electric carrier blocked by the blockers. To be consistent with this interpretation, the blocking factor variations are represented in Fig. 12 as a function of the matrix conductivity. The variation law is linear. According to this figure, the blocking effect would vanish when the matrix conductivity reaches about $3\times10^{-2}\Omega$. This is consistent with the observations on YSZ.[29]

Figure 13 shows the variations with the average grain size of the blocking factor for two measurement temperatures (350 and 450°C) and compares it with the corresponding YSZ data. The Y-TZP

Table 3. Activation energies and values at 350°C of the bulk conductivity

E_σ(eV)	*0·92 and 0·98*	*0·92*	*0·91(LT) 0·80(HT)*	*0·87(LT) 0·70(HT)*	*0·75(HT)*	*0·92*	*0·93*	*0·92*	*0·84*
σ350°C ($\times10^5$)	0·9	3·6	2·9	1·0	—	2·5	2·9	3 to 4	3·0
Ref.	5	6	7	19	20	13	21	15	This work

(HT), High temperature; (LT), Low temperature.

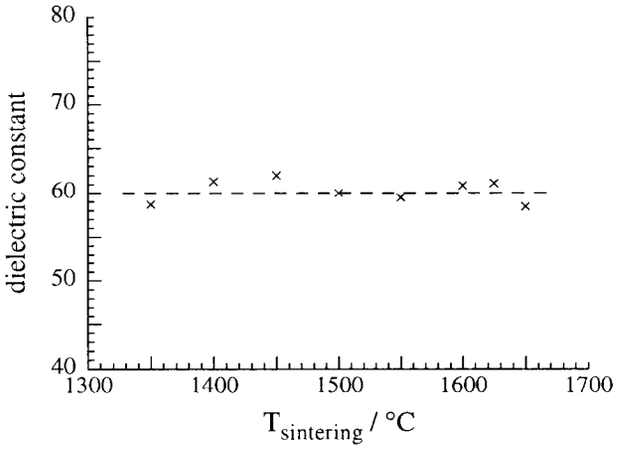

Fig. 9. Dielectric constant deduced from the bulk semicircle as a function of the sintering temperature.

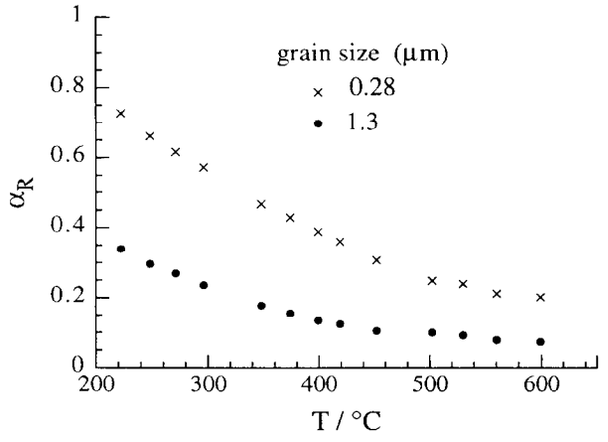

Fig. 10. Variations of the blocking factor as functions of the measurement temperature. (Samples sintered at 1350 and 1625°C.)

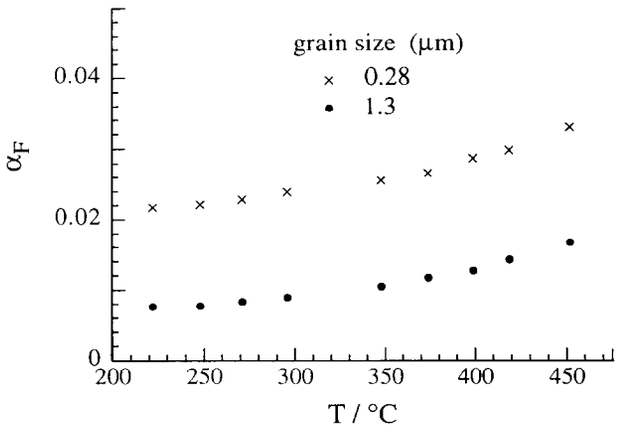

Fig. 11. Variations of the frequency ratio as functions of the measurement temperature. (Samples sintered at 1350 and 1625°C.)

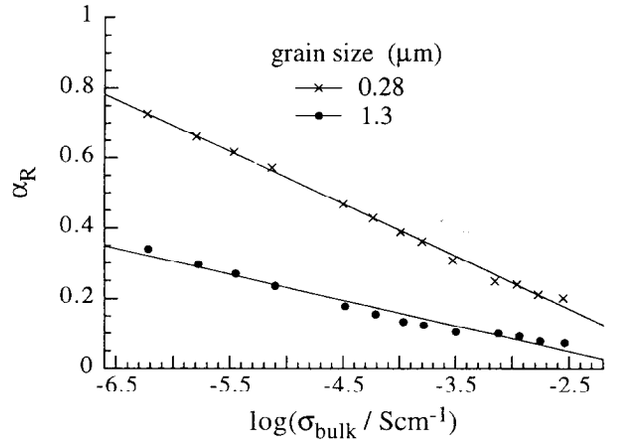

Fig. 12. Variations of the blocking factor as functions of the bulk conductivity (samples sintered at 1350 and 1625°C).

and YSZ values measured at 350°C are very similar. The Y-TZP slope does not depend on the measurement temperature and is slightly different from that of YSZ. The variation law is:

$$\alpha_R \approx (d_{50})^{-0.73}$$

The YSZ slopes previously reported[1] were −0·5 and −1.

Figure 14 compares the frequency factors. Here again, it can be noted that the variation law does not depend on the measurement temperature.

Figure 15 presents a more global comparison of the Y-TZP and YSZ data on an 'α_R versus α_C diagram'. This type of diagram has been found[1,34] useful to reveal transitions between different regimes where different families of blockers may dominate the blocking effect. Note that because of the variations of α_R and α_F with temperature, the comparison shown in this figure is strictly valid at the measurement temperature of 350°C only.

Two regimes can be distinguished: that of fairly constant α_C and that represented by the oblique lines. In a previous study,[1] the first one was identified as an intermediate regime where relatively flat voids, not fully 'resorbed' by the densification process, would still be present along the grain boundaries and

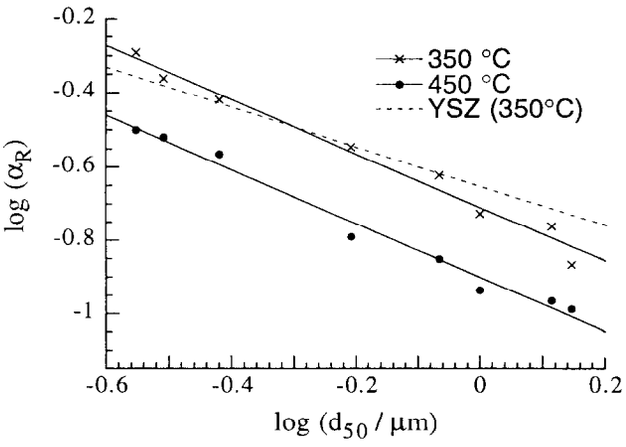

Fig. 13. Variations of the blocking factor with the average grain size. (Measurement temperatures: 350 and 450°C.) Comparison with results[1] obtained with YSZ at 350°C.

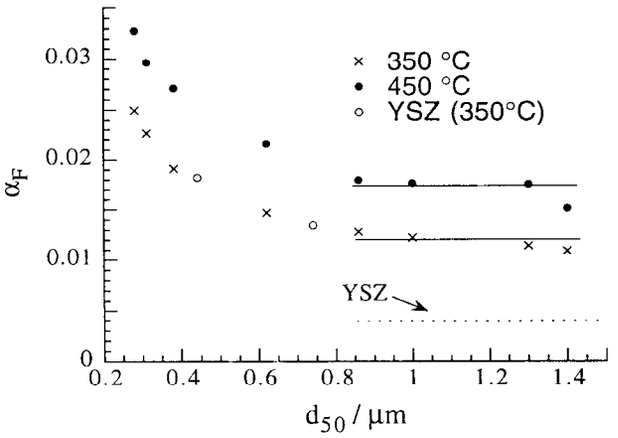

Fig. 14. Variations of 'the frequency ratio with the average grain size. (Measurement temperatures: 350 and 450°C.) Comparison with results[1] obtained with YSZ at 350°C.

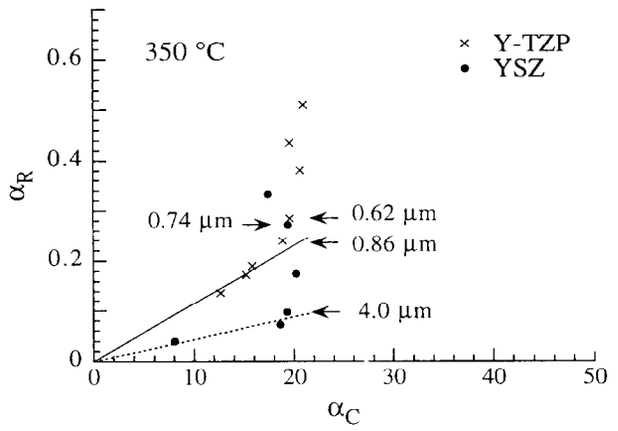

Fig. 15. α_R versus α_C diagram of the results. Comparison with YSZ[1]. (Measurement temperature: 350°C.)

would be the dominant blockers (in nominally pure materials). In this regime, the Y-TZP and YSZ examined here are very similar.

As the grains grow, the blocking effect would shift to a different regime,[1] called the intrinsic regime, represented by the oblique lines on the diagram. This intrinsic regime could be a sort of 'equilibrium state' for the grain boundaries. According to the results reported in the diagram, the transition to the intrinsic regime would occur at smaller grain sizes in Y-TZP. However, the number of experimental points which define the Y-TZP intrinsic regime in the diagram is unfortunately insufficient to fully support this conclusion.

5 Conclusions

For similar grain sizes (and similar impurity levels):

1. In many respects, the blocking effects in Y-TZP and YSZ appear surprisingly similar. This contrasts somewhat with the major difference between the grain growth activation energies.
2. In contrast to the behavior observed with YSZ, the blocking factor of Y-TZP (and correlatively its frequency factor) was found to decrease more rapidly with temperature from as low as 150°C.
3. The transition between the so-called intermediate regime, where micro-voids present along the grain boundaries would dominantly determine the blocking effect, and the intrinsic regime was observed to occur at smaller grain sizes in Y-TZP than in YSZ.

The analogies reported above suggest that, under conditions where the grain boundaries may play a significant role, especially under low loads,[34] the two materials could exhibit fairly similar mechanical properties. This should prompt a re-examination of the influence of the grain size on the mechanical properties of YSZ.

Acknowledgements

A. P. Santos acknowledges a grant from the Brazilian CNPq.

References

1. Steil, M. C., Thevenot, F. and Kleitz, M., Densification of yttria-stabilized zirconia; impedance spectroscopy analysis. *J. Electrochem. Soc.*, 1997, **144**, 390–398.
2. Muccillo, E. N. S. and Kleitz, M., Impedance spectroscopy of Mg-stabilized zirconia and cubic phase decomposition. *Journal of the European Ceramic Society*, 1996, **16**, 453–465.
3. Kuwabara, M., Ashizuka, M. Kubota, Y. and Tsukidate, T., Degradation of the electrical properties of Y_2O_3-partially stabilized zirconia ceramics owing to microcracking during annealing. *J. Mater. Sc. Let.*, 1986, **5**, 7–9.
4. Badwal, S. P. S. and Nardella, N., Formation of monoclinic Zirconia at the anodic face of tetragonal zirconia polycrystalline solid electrolytes. *Appl. Phys.*, 1989, **A49**, 13–24.
5. Bonanos, N., Slotwinski, R. K. Steele, B. C. H. and Butler, E. R., High ionic conductivity in polycrystalline tetragonal Y_2O_3–ZrO_2. *J. Mater. Sc. Let.*, 1984, **3**, 245–248.
6. Butler, E. P. and Bonanos, N., The characterization of ZrO_2 engineering ceramics by A. C. impedance spectroscopy. *Materials Sc. and Techn.*, 1985, **71**, 49–56.
7. Badwal, S. P. S. and Swain, M. V., ZrO_2–Y_2O_3: electrical conductivity of some fully and partially stabilized single grains. *J. Mater. Sc. Let.*, 1985, **4**, 487–489.
8. Badwal, S. P. S., Effect of dopant concentration on the grain boundary and volume resistivity of yttria–zirconia. *J. Mater. Sc. Let.*, 1987, **6**, 1419–1421.
9. Badwal, S. P. S. and Drennan, J., The effect of the thermal history on the grain boundary resistivity of Y-TZP materials. *Solid State Ionics*, 1988, **28–30**, 1451–1455.
10. Badwal, S. P. S. and Drennan, J., Grain boundary resistivity in Y-TZP materials as a function of the thermal history. *J. Mater. Sc.*, 1989, **24**, 88–96.

11. Badwal, S. P. S., Ciacchi, F. T. and Hannink, R. H. L., Relationship between phase stability and conductivity of yttria tetragonal zirconia. *Solid State Ionics*, 1990, **40–41**, 882–885.
12. Badwal, S. P. S., Yttria tetragonal zirconia polycrystalline electyrolytes for solid state electrochemical cells. *Appl. Phys.*, 1990, **A50**, 449–462.
13. Badwal, S. P. S., Ciacchi, F. T. Swain, M. V. and Zelizko, V., Creep deformation and the grain-boundary resistivity of tetragonal zirconia polycrystalline materials. *J. Am. Ceram. Soc.*, 1990, **73**, 2505–2507.
14. Badwal, S. P. S. and Drennan, J., Evaluation of conducting properties of yttria–zirconia wafers. *Solid State Ionics*, 1990, **40–41**, 869–873.
15. Badwal, S. P. S., Grain boundary resistivity in zirconia-based materials: effect of sintering temperatures and impurities. *Solid State Ionics*, 1995, **76**, 67–80.
16. Navarro, L. M., Marques, F. M. B. and Frade, J. R., Electronic and ionic domain of TZP: expected behavior and experimental results. In *Fourth EuroCeramics*, Vol. 5, ed. G. Gusmano and E. Traversa. Faenza Editrice Iberica, San Vincente, Spain, 1983, pp. 395-400.
17. Keizer, K. Van Hemert, M., Van de Graaf, M. A. C. G. and Burggraaf, A. J., Tetragonal zirconia: wet chemical preparation, mechanical and electrical properties. *Solid State Ionics*, 1985, **16**, 67–72.
18. Ikeda, S. Sakurai, O., Uematsu, K. Mizutani, N. and Kato, M., Electrical conductivity of yttria-stabilized zirconia single crystals. *J. Mater. Sc*, 1985, **20**, 4593–4600.
19. El Barhmi, A. Schouler, E. J. L. Hammou, A. and Kleitz, M., Electrical properties of tetragonal partially stabilized zirconia. In *Science and Technology of Zirconia III*, ed. S. Somiya, N. Yamamoto and H. Yanagida, The American Ceramic Society, Columbus, OH, 1988, pp. 885–894.
20. Yamamoto, O., Takeda, Y. Kanno, R., Kohno, K. and Kamiharai, T., Electrical conductivity of polycrystalline tetragonal zirconia ZrO_2–M_2O_3 (M = Sc, Y, Yb). *J. Mater. Sc. Let.*, 1989, **8**, 198–200..
21. Gödickemeier, M., Michel, B., Orliukas, A., Bohac, R, Sasaki, K. and Gaukler, L., Effect of intergranular glass films on the electrical conductivity of 3Y-TZP. *J. Mater. Res.*, 1994, **9**, 1228–1240..
22. Whalen, P. J, Reidinger, R, Correale, S. T. and Marti, L., Yttria migration in Y-TZP during high-temperature sintering. *J. Mater. Sc.*, 1987, **22**, 4465–4469.
23. Theunissen, G. S. A. M, Winnubst, A. J. A. and Burggraaf, A. J., Segregation aspects in the ZrO_2–Y_2O_3 ceramic system. *J. Mater. Sc. Let.*, 1989, **8**, 55–57.
24. Hwang, S.-L. and Chen, I.-W., Grain size control of tetragonal zirconia polycrystals using the space charge concept. *J. Am. Ceram. Soc.*, 1990, **73**, 3269–3277.
25. Hughes, A. E. and Badwal, S. P. S., Impurity and yttrium segregation in yttria–tetragonal zirconia. *Solid State Ionics*, 1991, **46**, 265–274.
26. Theunissen, G. S. A. M, Winnubst, A. J. A. and Burggraaf, A. J., Surface and grain boundary analysis of doped zirconia ceramics studied by AES and XPS. *J. Mater. Sc.*, 1992, **27**, 5057–5066.
27. Syed Asif, S. A., Muthu, A. V. D., Sood, A. J. and Biswas, S. K., Surface damage of yttria-tetragonal zirconia polycrystals and magnesia-partially-stabilized zirconia in single point abrasion. *J. Am. Ceram. Soc.*, 1995, **78**, 3357–3362.
28. Dessemond, L., Muccillo, R. Henault, M. and Kleitz, M., Electrical conduction-blocking effects of voids and second phases in stabilized zirconia. *Appl. Phys.*, 1993, **A57**, 57–60.
29. Kleitz, M., Dessemond, L. and Steil, M. C., Model for ion-blocking at internal interfaces in zirconias. *Solid State Ionics*, 1995, **75**, 107–115.
30. Groot Zevert, W. F. M., Winnubst, A. J. A., Theunissen, G. S. A. M. and Burgraaf, A. L., Powder preparation and compaction behavior of fine-grained Y-TZp. *J. Mater. Sc.*, 1990, **25**, 3449–3455..
31. Bourell, D. L., Parimal and Kaysser, W., Sol–gel synthesis of nanophase yttria-stabilized tetragonal zirconia and densification behavior below 1600K. *J. Am. Ceram. Soc.*, 1993, **76**, 705–711..
32. Shi, J. L., Ruan, M. L. and Yen, T. S., Crystallite growth in yttria-doped superfine zirconia powders and their compacts. A comparison between Y-TZP and YSZ. *Ceramics Intern.*, 1996, **22**, 137–142.
33. Sagel-Ransijn, C. D., Winnubst, A. J. A., Kerkwijk, B., Burggraaf, A. J. and Verweij, H., Production of defect-poor nanostructured ceramics of yttria–zirconia. *Journal of the European Ceramic Society*, 1997, **17**, 831–841.
34. Kleitz, M., Pescher, C. and Dessemond, L., Impedance spectroscope of microstructure defects and crack characterization. In *Science and Technology of Zirconia V*, ed. S. P. S. Badwal, M. J. Bannister and R. H. J. Hannink. Technomic, Lancaster–Basel, 1993, pp. 593–608.